Eur. Phys. J. B **1**, 491–501 (1998)

THE EUROPEAN PHYSICAL JOURNAL B

Structural and dynamical properties of aqueous suspensions of NaPSS (HPSS) at very low ionic strength

St. Batzill, R. Luxemburger, R. Deike, and R. Weber[a]

Fakultät für Physik, Universität Konstanz, Postfach 5560, 78464 Konstanz, Germany

Received: 5 May 1997 / Revised: 1 September 1997 / Accepted: 10 November 1997

Abstract. Results on the structural and dynamical properties of aqueous solutions of NaPSS (HPSS) are reported. Most samples of previous measurements, including our own, are contaminated by the presence of (temporal) aggregates. The emphasis of this paper lies on investigations of well purified samples at very low ionic strength where interacting effects are maximum. As previously reported, this can be achieved by pumping the suspension through ion exchange resin by means of a tube-pump, using filters of 0.1 μm pore size. Information has been extracted from static and dynamic light scattering and viscosity measurements. A second maximum is observed in the scattering curves *versus* wavenumber for the first time. It is discussed on the basis of two current models describing the structure of charged macromolecules. The short time dynamics reflects the measured intensity. Detailed viscosity data in comparison of those of rodlike (TMV), slightly flexible so-called fd *virus* particles (length 880 nm) are used to confirm the interpretation of the light scattering results. The recently observed maximum in the reduced viscosity could be confirmed.

PACS. 51.20.+d Viscosity, diffusion, and thermal conductivity – 78.35.+c Brillouin and Rayleigh scattering; other light scattering – 82.70.Kj Emulsions and suspensions

1 Introduction

The structural and dynamical properties of highly charged polyelectrolytes at low ionic strength have been the subject of many investigations [1]. Especially aqueous solutions of sodium polystyrenesulphonate has served as a model system. Small angle neutron scattering (SANS) was the first technique which revealed a broad intensity maximum [2], that later was compared to the reciprocal effective diffusion coefficient derived from neutron spin echo measurements [3,4]. Since then, various papers have appeared that dealt with the properties of NaPSS solutions [1]. Whereas SANS and SAXS- (small angle X-ray scattering) techniques [5,6] are best suited to explore the properties of semidilute/concentrated solutions (depending on the molecular weight (MW) of the samples used), light scattering (LS) monitors the dilute/semidilute regime. Typical concentrations range around 0.01 mg/ml compared to about 50 mg/ml with the former techniques. The first static and dynamical LS investigations are due to Drifford *et al.* [7]. Again a single maximum in scattered intensity was observed. In two recent articles we have extended the LS measurements arriving at equivalent results [8,9]. It should be mentioned that a similar feature was observed for other polyelectrolytes [1]. Theoretically, the maximum observed in SANS and SAXS has been described by an isotropic model based on a correlation hole concept [10].

Careful sample preparation is of high significance. It has been recognized that NaPSS tends to form steady or temporal aggregates visible as a strong intensity increase at small wavenumbers [1,7–9]. It cannot be excluded that they also influence the static structure factor of the solution. The dynamics are severely affected by these aggregates too as a so-called slow mode occurs [11]; this mode has been claimed to be absent in pure samples [12], but this is still a matter of debate [1]. Subsequently Gosh *et al.* have shown that these features can be eliminated by pressing the solution through a filter of at most 0.1 μm pore size [12]. Since this condition was not met in our previous investigations as well as in other ones we have resumed LS measurements on aqueous solutions of NaPSS. Emphasis is put on highly interacting samples as described below.

In a second step we have investigated the short time behaviour of the correlation function which we have compared with the results of the static measurements, and finally we report on detailed viscosity measurements. Various investigations of this type have already been reported, which, however, come to different conclusions [13–16]. In some papers, the ionic strength was not minimum or the shear rate dependence was not measured [13]. Our results can be used to qualitatively support statements of SLS measurements concerning the conformation of the chains.

[a] e-mail: Reinhart.Weber@uni-konstanz.de

2 Experimental

Sodium polystyrenesulphonate was purchased by Polysciences Europe. In order to investigate polyelectrolytes with different contour lengths L_c the following molecular weights were used: MW = 183 kg/mol (L_c = 222 nm), MW = 356 kg/mol (L_c = 432 nm), MW = 744 kg/mol (L_c = 903 nm), MW = 1010 kg/mol (L_c = 1226 nm), MW = 2870 kg/mol (L_c = 3483 nm). According to the manufacturer, the polydispersity of the salt form is characterized by $M_W/M_n \leq 1.1$ (≤ 1.2 for MW 2870 kg/mol), and the degree of sulphonation larger than 90%. The preparation of salt free samples was achieved by a well known procedure used for obtaining saltfree suspensions of spherical or rodlike particles [17] which differs from the preparation of NaPSS samples for SANS and SAXS experiments. First, for each molecular weight, a stock suspension was prepared by dissolving the weighted salt in carefully deionized water ($R > 18$ MΩ). The process of purification and deionizing of the appropriate concentrated samples was then accomplished in a closed circuit using a tube-pump to circulate the suspension through a mixed bed ion ex-change resin [17,18]. Conductivity measurements yielded a charge density per monomer of about 0.25. Almost all the Na^+ counterions are exchanged by H^+ which was confirmed by pH measurement. In what follows, we note the molecular weights of NaPSS. As mentioned above, cleaning from precipitates was achieved by a millipore filter of 0.1 μm pore size. In our previous investigations the pore size was 1.5 μm. The concentration was measured with a Beckman spectrometer DM 64 at the absorption maximum (λ = 224 nm) after completion of the light scattering or viscosity measurement. For neutron scattering measurements after purification by ion resins, the polyelectrolyte was neutralized with sodium hydroxide and then lyophilized. The ionic strength of those samples will not be quite as low as that of our samples at small concentrations. Since most of the Na^+ ions are replaced by H^+ ions, these solutions represent almost pure two-component systems. The self ionization of water is suppressed [1,19] and therefore essentially no coions are present in the solution. In contradiction, NaPSS solutions can hydrolyse. Although NaPSS derives from a strong acid, ion exchange can take place between the Na^+ counterions and water, leading to the formation of small amounts of NaOH. These solutions contain therefore small amounts of salt.

We used commercial light scattering equipment (ALV 5000, Langen/Germany) consisting of a computer controlled goniometer table with focusing and detector optics, a power stabilized 3 W argon laser (Spectra Physics), a digital rate meter and a temperature control, stabilizing the temperature of the sample cell at ±0.1 °C [8]. For the viscosity experiments a computer controlled Couette type rotational viscosimeter (Contraves Low Shear 40, Fa. Mettler) was employed. It allows measurements in the range of 1 mPas (water) at a shear rate of $\dot{\gamma} = 0.5\ s^{-1}$ with an accuracy of better than 3%. The measuring system was flushed by nitrogen gas to get samples of lowest ionic strength. The sample was again kept in the closed pump circuit. Connection to the viscosimeter vessel was made by two glass pipettes [20]. The whole apparatus was first thoroughly cleaned by pumping highly purified water through it. A minimum conductivity of 0.6 and of 70 μS/cm was achieved with samples of lowest and highest concentration, respectively. During the measurement the conductivity raised only by a few percent.

3 Static and dynamic light scattering

Information on the shape of the single macroparticle is contained in the form factor $P(q)$ where q is the scattering vector. The mutual arrangement of the chains is given by the structure factor $S(q)$. The scattering intensity can formally be written as the product of the form factor $P(q)$ and the static structure factor $S(q)$. If the particles are flexible as is the case for NaPSS, only a mean value for the single particle form factor can be given. As long as there is no interaction between the chains, $S(q)$ is equal to one and the form factor can experimentally be determined. However, this becomes impossible when the chains are charged. Indeed changes of form result from the repulsion of neighboring segments leading to some stretching of the macroparticles. Thus, the form factor changes, but only the product $S(q)\,P(q)$ can be measured. In contrast to the situation with rodlike particles, only the scattering intensity can be plotted. We are mostly interested in the structure in the semidilute region. For this purpose, MW's of 744 kg/mol (Fig. 1a) and 1010 kg/mol (Fig. 1b) are well suited. The transition between the dilute and the semidilute regime is defined here by the concentration dependence of the wavenumber of the main maximum, q_{max}, changing from

$$q_{max} \propto c^{1/3} \quad \text{to} \quad q_{max} \propto c^{1/2} \quad \text{as explained later.}$$

As can be derived from Figure 2, the transition takes place between $c = 1.5c_c^*$ and $c = 2.5c_c^*$. Here $c_c^* = 1\ \text{particle}/L_c^3$ where L_c is the contour length. Consequently, the first MW 744 sample refers to the transition regime where the other one and all three MW 1010 samples are located in the semidilute regime. Besides the well known first peak, a second maximum is clearly visible, which would even be more pronounced if $S(q)$ could be plotted, since the (unknown) form factor decreases with increasing q. For smaller MW's the intensity is too weak to be resolved from the background. The large intensity increase towards small wavenumbers mentioned above and observable in previous publications does not occur here or is very much reduced, which means that aggregates are essentially absent.

An oscillatory behaviour of $I(q)$ and $S(q)$ is known to appear for aqueous suspensions of rodlike and weakly flexible particles. Extensive experimental studies have been performed mainly on suspensions of charged tobacco mosaic viruses (TMV, length 300 nm) and so called fd viruses (length 880 nm) [21,22]. Detailed theoretical treatments are available showing a liquid like order of the particles below the overlap concentration $c^* = 1\ \text{particle/length}^3$

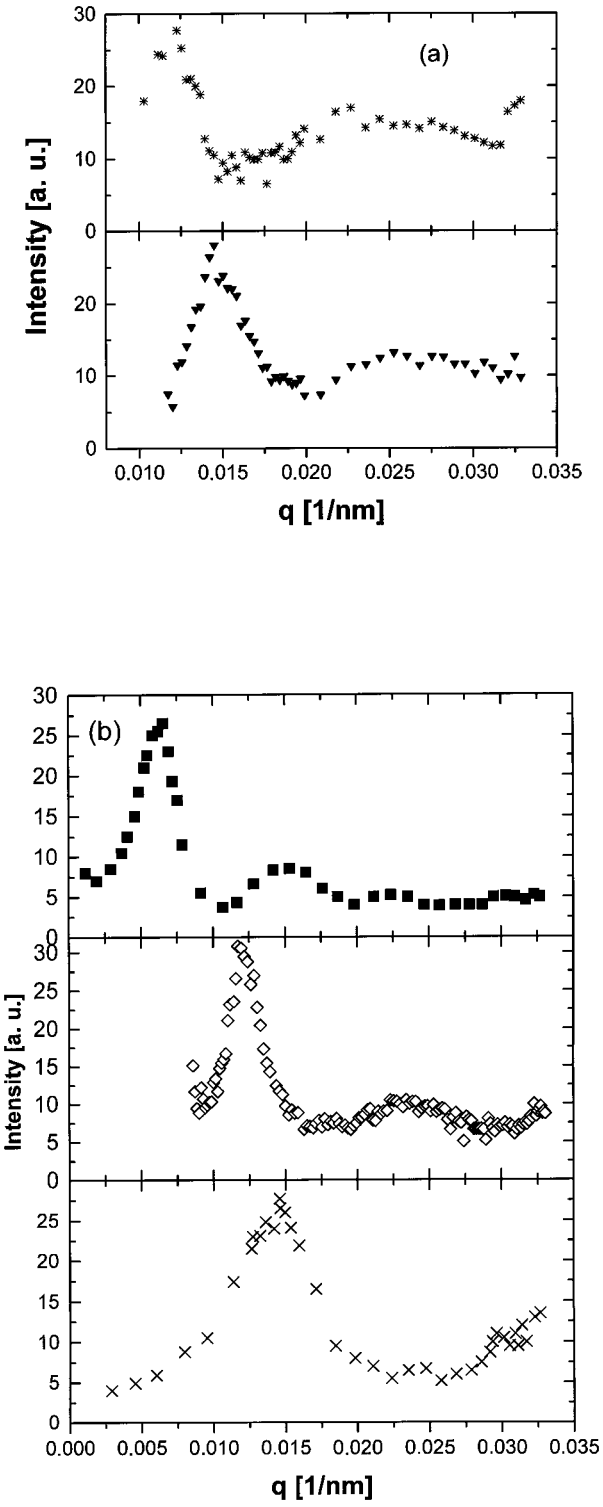

Fig. 1. (a) Scattering intensity *versus* wavenumber. MW = 744 kg/mol: c = 0.0042 mg/ml (∗) and c = 0.0067 mg/ml (▼). (b) Scattering intensity *versus* wavenumber MW = 1010 kg/mol: c = 0.004 mg/ml (■); c = 0.0063 mg/ml (◇); $c = 0.011$ mg/ml (×).

[23,24]. It is expressed in $S(q)$ by that part of the structure factor which arises from the center-to-center correlations only. However, at about $4c^*$, this peak vanishes. The total $S(q)$ has still a peak because of the angular correlations between the particles, which become important at about c^* and above. Globally no orientational order exists. The concentration dependence of $q_{\max}$ changes from $c^{1/3}$ to $c^{1/2}$ around c^* [1]. Good agreement has been found between experimental [23] and theoretical results [21,22].

Because of the flexibility of the macroparticles, this model can only be applied with circumspection. We put it aside while describing another model, which has been applied successfully to the single maximum found in neutron- and X-ray investigations of flexible chains. This is called the isotropic model, applicable in the semidilute regime. Here, the chains are entangled and form an isotropic transient network. The structure is described by a dense assembly of blobs of size ξ. At length scales smaller than ξ, electrostatic interactions lead to a rodlike conformation of the chains. For scales larger than ξ, the interactions are screened out and each chain behaves randomly. The structure factor resembles the so called correlation hole first introduced by de Gennes in polymer melts [25]. The model is characterized by a broad peak in the scattered intensity. More detailed calculations have been done meanwhile, which show a single peak as consequence of the correlation hole [26–29]. No oscillatory behaviour of the intensity has been derived so far.

In the semidilute regime, all model calculations essentially predict a concentration dependence of $q_{\max}$ proportional to $c^{1/2}$. According to the liquid like picture for $c \ll c_c^*$, $q_{\max}$ has to vary proportional to $c^{1/3}$ since in this case it is approximately a measure of the reciprocal mean distance between centers of gravity, as already mentioned. Thus, we are able to estimate a mean length L_{eff} from the experimental data of Figure 2. Here, the product of $q_{\max}$ by the contour length is plotted *versus* the concentration normalized to the overlap concentration c_c^*, defined above in a logarithmic representation. In this way, all LS data of $q_{\max}$ for different MW's below c_c^* and above $2.5c_c^*$ respectively, can be found each on a straight line as in the case of rodlike particles. The best fit in the semidilute regime is obtained by an exponent of 0.47, but to a good approximation, the results can be described by

$$q_{\max} L_c = a \left(\frac{c}{c_c^*} \right)^{1/2}, \; a = 1.0$$

as can be seen from the additional line in Figure 2.

Using for c the value $2.0c_c^*$ one arrives at $L_{\text{eff}} \approx 0.8 L_c$. This means that the chains are not Gaussian coils but are fairly stretched at these concentrations. What is important is not the absolute number of L_{eff} but the fact that the crossover from an exponent of 1/3 to 1/2 takes place not much above c_c^*. At higher concentrations, due to the increasing ionic strength, stronger coiling may occur compatible with computer simulations on short chains [30].

[1] This finding agrees closely with the overlap concentration observed previously, if only the light scattering results are taken into account [9].

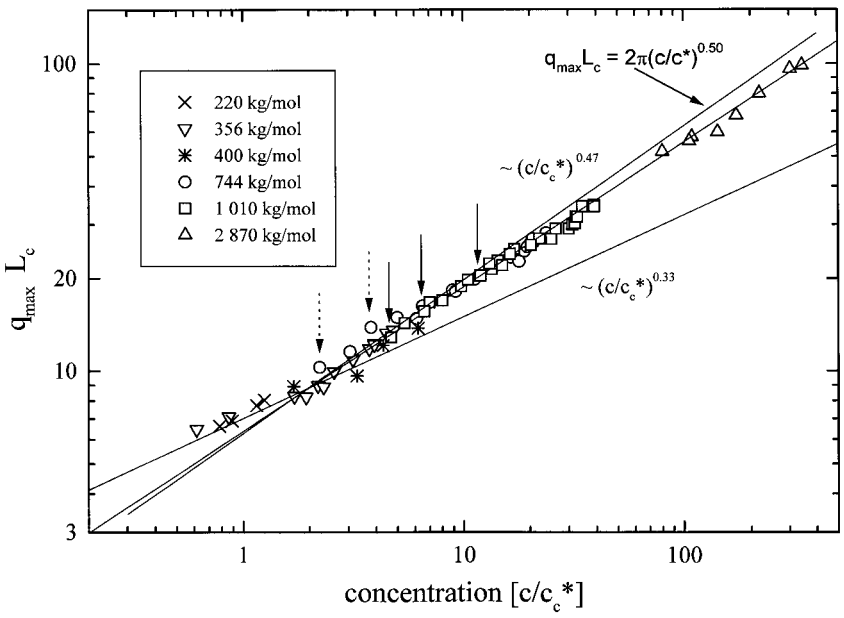

Fig. 2. Wavenumber of the first intensity maximum multiplied by the contour length L_c *versus* concentration normalized to $1/L_c^3$ for various molecular weights. 220 kg/mol (×), 356 kg/mol (▽), 400 kg/mol (∗), 744 kg/mol (o), 1010 kg/mol (□), 2870 kg/mol (△). The points marked by arrows correspond to the samples of Figures 1a, 1b.

Further extraction of the conformation of the chains are not possible at present. Application of the model for rodlike particles is questionable because of the nonnegligible flexibility of the (charged) chains. The isotropic model on the other side, as far as it has been worked out, does not show oscillatory behaviour.

4 Short time dynamics

For solutions of spherical particles it has been shown both theoretically and experimentally that the reciprocal short time diffusion coefficient $D_i(q)$ is given by the structure factor divided by the diffusion coefficient D_o of noninteracting spheres provided by hydrodynamic interactions are neglected [31]

$$\frac{1}{D_i(q)} = \frac{S(q)}{D_o}\,. \tag{1}$$

It has been proved experimentally that this relation holds also for rodlike particles even in the semidilute regime if D_o and D_i are replaced by effective diffusion coefficients $D_{\mathrm{eff},0}(q)$ and $D_{\mathrm{eff},i}(q)$, respectively. They reflect all different types of motion of the particles in the scattering volume such as translational, rotational and bending modes. For flexible polyelectrolytes the first LS results of Drifford *et al.* [7] on samples of MW 7.8×10^5 indicate a similar behaviour. Neutron spin echo measurements reveal only partial agreement [4]. Therefore, to establish the relation between structural order and diffusive behaviour, we have performed detailed dynamical light scattering investigations on solutions of four molecular weights.

The effective diffusion coefficient is derived from the field correlation function of the scattered light which is related to the measured intensity correlation function by the Siegert relation [32].

$$g_I(q,t) = \langle I(q,0)I(q,t)\rangle/\langle I(q)\rangle^2 \tag{2}$$

$$g_E(q,t) = \langle E(q,0)E(q,t)\rangle/\langle I(q)\rangle. \tag{3}$$

The field correlation function reflects all different types of motion mentioned above. In the absence of an adequate theory it is not possible to calculate $g_E(q,t)$ for a given flexible particle in the case of strong interparticle interaction. Therefore there is no way to determine the correspondent diffusion coefficients in an unequivocal and consistent manner. Of course the experimental data can be fitted by a sum of several exponential functions, but there exists no method to connect the relaxation times with a special kind of single particle motion. Nevertheless, a well-defined quantity is represented by the first cumulant

$$K_1(q) = -\frac{\mathrm{d}}{\mathrm{d}t}\{\ln g_E(q,t)\}_t \tag{4}$$

which can be related to an effective diffusion coefficient *via*

$$D_{\mathrm{eff}}(q) = K_1(q)/q^2. \tag{5}$$

To study the short time behaviour of the field correlation function in interacting solutions of *rodlike* particles, use has been made of an equation that was originally derived for strongly interacting spheres [31], given by

$$K_{1,i}(q) = K_{1,0}(q)/S(q). \tag{6}$$

This means that the first cumulant $K_{1,i}(q)$ can be calculated from the first cumulant of suspensions of noninteracting particles, $K_{1,0}$, and the static structure factor $S(q)$. Using the above equation one gets

$$S(q) = D_{\mathrm{eff},0}(q)/D_{\mathrm{eff},i}(q) \tag{7}$$

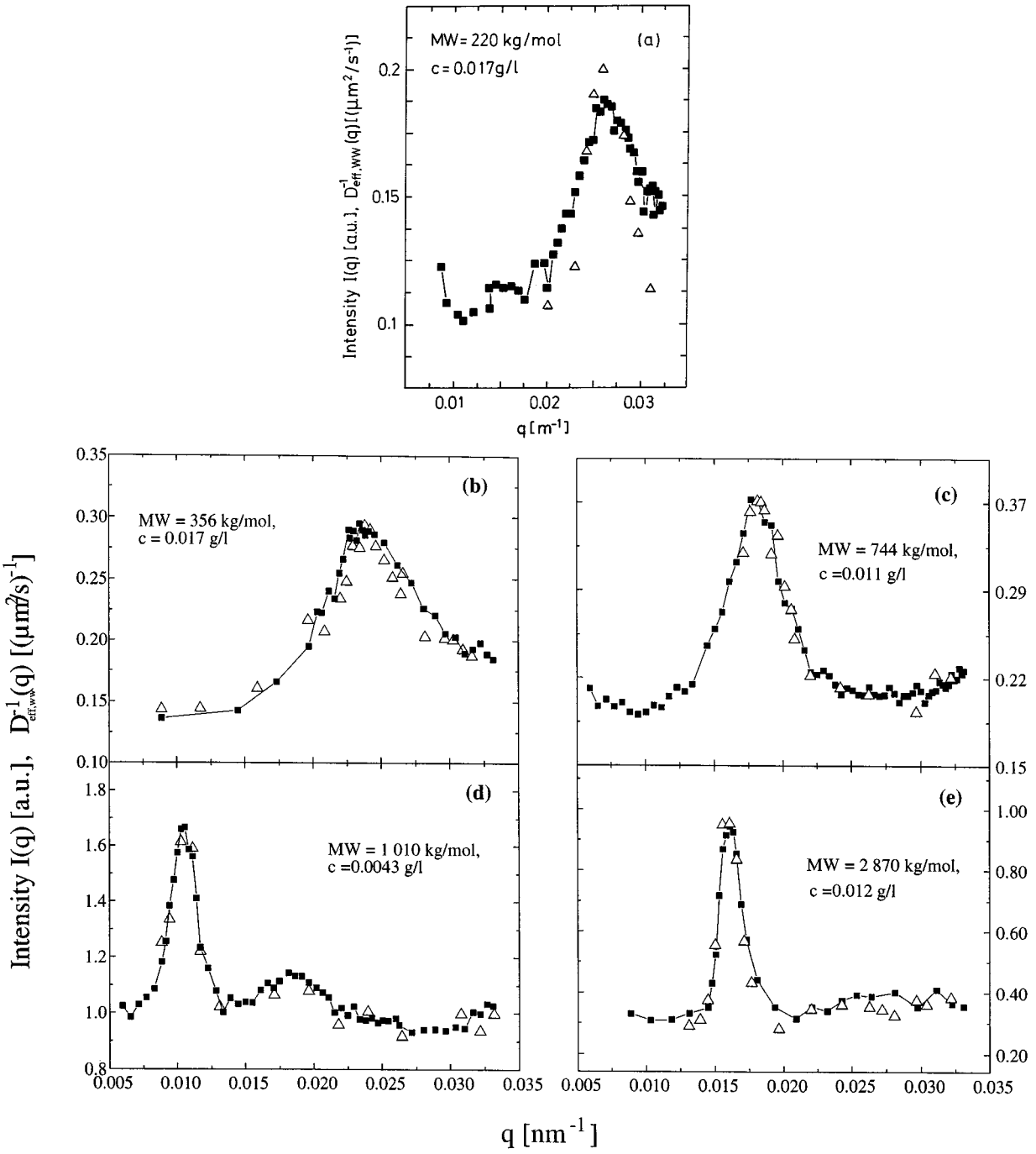

Fig. 3. Comparison between the scattering intensity (■) and the reciprocal effective diffusion coefficient (△) *versus* wavenumber.

where $D_{\mathrm{eff},0}(q)$ denotes the effective diffusion coefficient for noninteracting particles introduced above. Since it is in general only a weak function of q, the relation shows that high structural order is accompanied by a strong slowing down of the diffusion.

For flexible particles equation (7) cannot be applied, since only the measured intensity is accessible. Therefore we write instead

$$I(q) = \frac{D_{\mathrm{eff},0}(q)P(q)}{D_{\mathrm{eff},i}(q)} \,. \tag{8}$$

The theory assumes that the shape of the particles remains unchanged when the interaction is switched on. As already mentioned, this is not fulfilled for flexible particles. Therefore, one can only compare $I(q)$ with $1/D_{\mathrm{eff},i}(q)$. This is done in Figures 3a-f. By fitting both curves at $q_{\max}$, good agreement is obtained, which indicates that

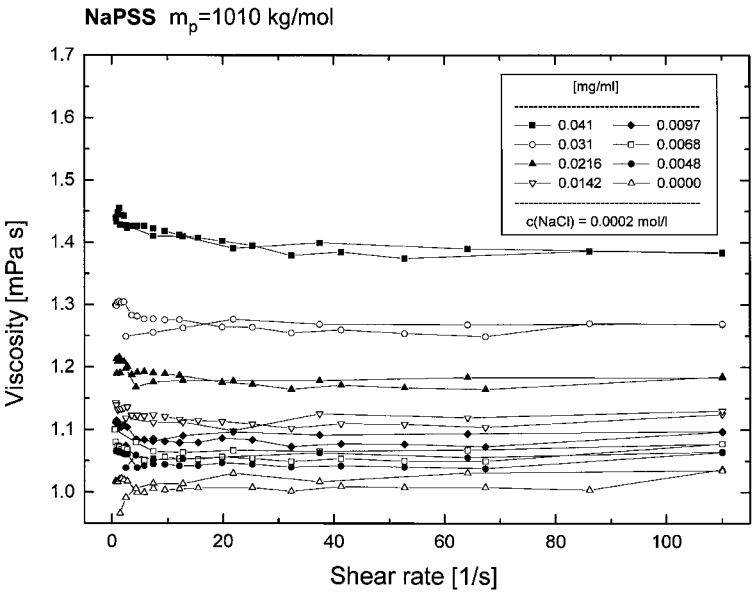

Fig. 4. Viscosity of aqueous suspensions of NaPSS (MW 1010 kg/mol) with added salt for different concentrations as given in the inlet.

the nominator is essentially constant. For the lowest MW = 220 kg/mol because of the weak scattering power, the results are affected by rather big errors. As is obvious from Figure 3d, also the second maximum is reproduced in $1/D_{\mathrm{eff},i}$. Therefore, on the whole, for all MW's the data confirm the proportionality between $I(q)$ and $1/D_{\mathrm{eff},i}(q)$ At not too high concentration, it is tempting to interpret this as a consequence of a liquid like order of the particles.

It is interesting to compare our results with those of spin echo investigations of Kanaya *et al.* [4] at four orders of magnitude higher concentrations but similar molecular weights. Good agreement is found there only at wavenumbers below that of the maximum of $I(q)$. Around $q_{\max}$ and above the reciprocal effective diffusion coefficient is flatter than the intensity $I(q)$.

5 Viscosity

The viscosity reflects the shape of the macroparticles, their flexibility and mutual arrangement. These properties strongly depend on the electrostatic interaction of the polyions. Therefore, viscosimetry can be used, besides light scattering, to learn something about these properties.

There exists already a variety of papers dealing with the viscosity of NaPSS [13–16]. In all cases, a maximum of the reduced viscosity is observed as function of concentration (Fig. 5). Its position, c_{pmax}, and magnitude depend only slightly on the molecular weight of the samples. Increasing the ionic strength by adding small amounts of salt results in a rise of c_{pmax} by more than one order of magnitude before vanishing. Vink has compared his viscosity data of NaPSS solutions with those of HPSS and found that c_{pmax} decreases by about 30%. He attributed this difference to the smaller ionic strengths of the HPSS samples at small concentrations as explained in the experimental part. Anticipating our data in Figure 5 this might in part

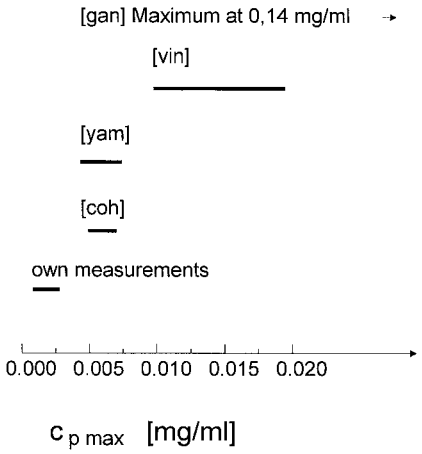

Fig. 5. Spreading of the position of the maximum of reduced viscosity of comparable molecular weights obtained by various authors, Coh [13], Yam [14], Vin [15], Gan [16].

explain the shift of c_{pmax} towards somewhat smaller concentrations. Finally, for a quantitative comparison of the different results, it has to be taken into account that the shear rate dependence could not always be examined since a capillary viscosimeter was used [13].

It was our intention again to add results on very pure samples at minimum ionic strength.

At first we demonstrate the big increase of the viscosity when the salt is removed from the solution. This is demonstrated in Figures 4 and 6a which show viscosities at high and small ionic strengths, respectively, for MW = 1010 kg/mol. In the latter case, the zero shear values are about an order of magnitude bigger. Figures 6a-d show the results for different molecular weights. The viscosity *versus* the shear rate is plotted. The zero shear

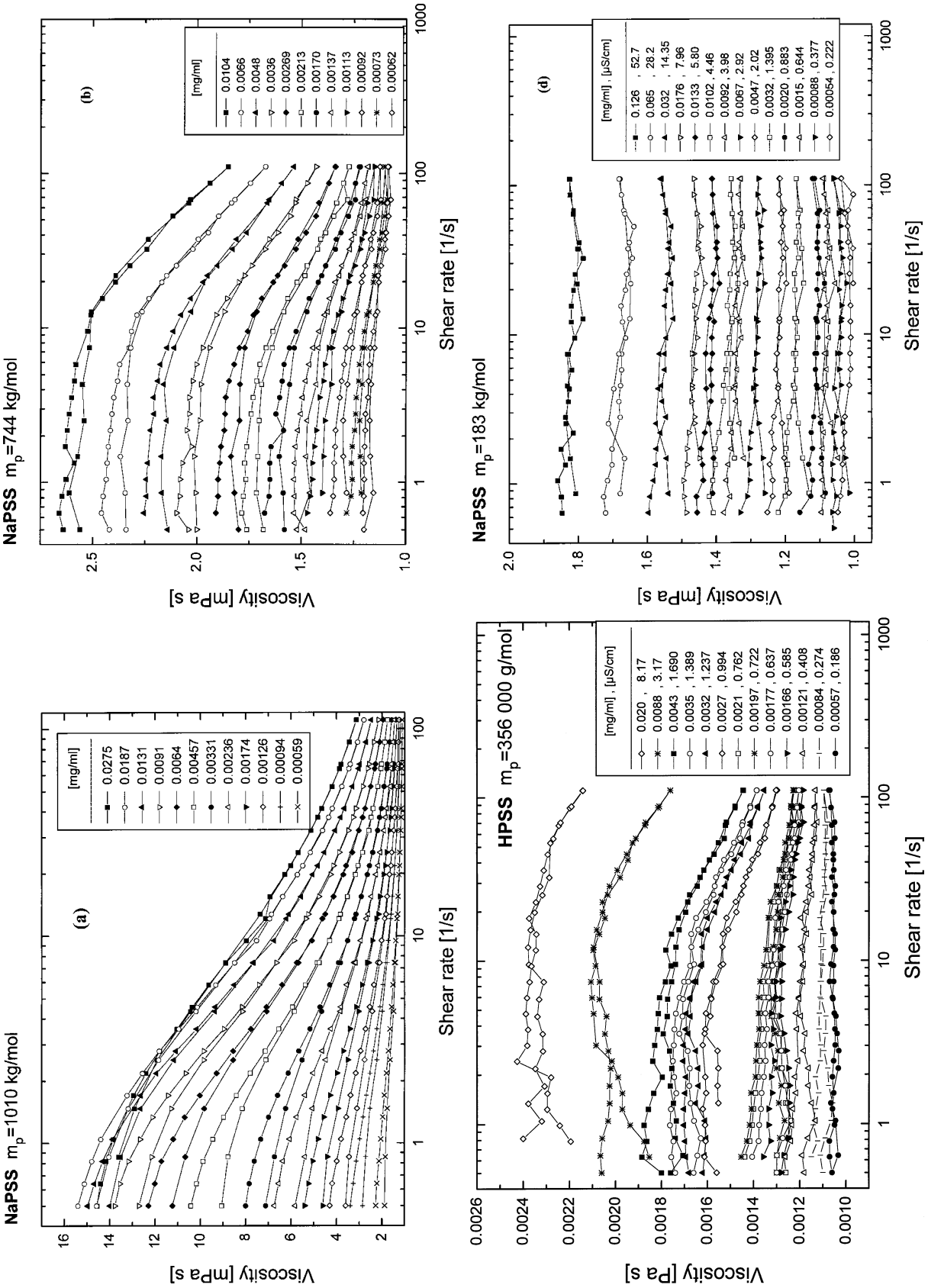

Fig. 6. Viscosity of aqueous suspensions of NaPSS at low ionic strength as function of shear rate for various concentrations as given in the inlet: a) MW 1010 kg/mol, b) MW 744 kg/mol, c) MW 356 kg/mol, d) MW 183 kg/mol.

rate values taken at the same monomer concentration increase by almost a factor of ten by raising the MW from 183 kg/mol to 1010 kg/mol. A weak shear rate dependence sets in for MW = 356 kg/mol at $\dot{\gamma} = 10\ s^{-1}$. The measurements refer to the dilute regime below c_c^*. They may be compared to the viscosities of rodlike TMV with a length of 300 nm [33], ranging within the contour lengths of our NaPSS particles. In this case, the viscosity does not depend on the shear rate. Its absolute value is very similar to the mean value of the zero shear viscosities of the NaPSS samples defined above at comparable particle concentration.

As expected, for higher molecular weight samples, the shear rate dependence increases. Strong shear thinning is observed for particles of MW = 1010 kg/mol. Samples of MW = 744 kg/mol have a contour length of 903 nm. It is therefore again interesting to compare their viscosities with those of slightly flexible fd-particles of length 880 nm [34]. It turns out that the zero shear values and the shear rate dependence are again similar; the PSS solutions behave like suspensions of only little shorter rods. No peculiar change of the viscosity is observed by raising the concentration through c_c^* or some nearby value. Because of the similarities stated, we again conclude that the shape of these NaPSS particles are not far from being rodlike at small ionic strength, in agreement with the light scattering and recent birefringence results [9].

The concentration dependence of the viscosity is plotted in Figures 7a-d. The curves increase linearly first, then bend towards a constant value when the concentration gets much bigger than the overlap concentration c_c^*.

Finally, the reduced viscosity, defined as

$$\eta_{\mathrm{red}} = \frac{\eta - \eta_s}{\eta_s c_p} \tag{9}$$

is shown for four molecular weights. η_S is the viscosity of pure water in our case. As already mentioned, it exhibits a maximum at a concentration almost independent of molecular weight [13–16]. According to our measurements, it is located at $c = (1.6 \pm 0.2) \times 10^{-3}$ mg/ml, slightly below the values reported so far. The maximum is most pronounced for the highest molecular weight samples. For MW 1010 kg/mol overlap of the chains occurs for most of the concentrations according to the LS results, whereas for MW 744 kg/mol the highest concentrations are in the transition regime. The particles of the two lowest molecular weight samples of Figures 6c, d on average stay far away from each other, $c/c_c^* \ll 1$.

The appearance of a maximum seems typical of flexible polyelectrolytes. It has also been found for particles of other chemical composition (for ref. see [19]), but we have not observed it for macromolecules of rodlike shape. For example, for TMV η_{red} is a decreasing function of concentration [33], whereas for the slightly flexible fd-particles it is about constant[2] at small concentrations and then also decreases. It has been argued that because of the very low concentration artifacts like adsorption at the walls might lead to a maximum in η_{red}, but the effect was found to be too small [14]. Cohen and Priel have applied a theory of Hess and Klein [35], originally derived for interacting spherical particles. Therefore they had to limit their considerations to the dilute regime. However, it remains unclear on which physical grounds the maximum occurs. Since the effect is not observed for rodlike particles, it seems reasonable to correlate it to conformational changes occurring during dilution of the suspension. The ionic strength C_s is given by [19]

$$C_s = c_a + \varepsilon c_p \tag{10}$$

where ε characterizes the degree of dissociation of the counterions and how the add to the suspensions effective ionic strength, c_a is the amount of salt.

When c_p decreases C_S decreases too. According to Reed [19], lowering C_s leads to an expansion of the polyelectrolyte coils at such a rate that the square of the viscometric volume occupied by a given macromolecule increases faster than c_p decreases, thus leading to an increase in η_{red}. As c_p decreases further, the chains will approach their maximum size, and therefore the viscometric volume will become independent of c_p and c_s, and the reduced viscosity decreases, giving rise to a maximum. The shape of the curves depends on the particular model to calculate $[\eta]$. In spite of this plausible explanation, caution has to be taken since Yamanaka *et al.* [14] have reported a maximum also to exist in aqueous suspensions of spheres whose shape does not change with concentration.

6 Summary

Light scattering measurements on carefully prepared aqueous solutions of NaPSS (HPSS) at very low ionic strength have revealed for the first time a q dependent oscillating intensity, equivalent to that which has been found recently for suspensions of rodlike and weakly flexible macroparticles. The wavenumber of the maximum varies at $c^{1/3}$ below a certain overlap concentration close to $2c_c^*$ and as $c^{0.47}$ above it. From this a mean length of the chains around those concentration of $L \approx 0.8 L_c$ (L_c contour length) can be estimated. Low shear viscosity measurements were compared to those of suspensions of rodlike TMV and semiflexible fd-particles. The results are consistent with the fact that the polyelectrolyte chains are rather stretched. The reduced viscosity shows a pronounced maximum at a very low concentration in fair agreement with existing data on aqueous solutions of HPSS and NaPSS. It might originate in the change of the shape of the macromolecules with decreasing concentration.

[2] Data are somewhat incomplete, since they have been taken at a few concentrations only.

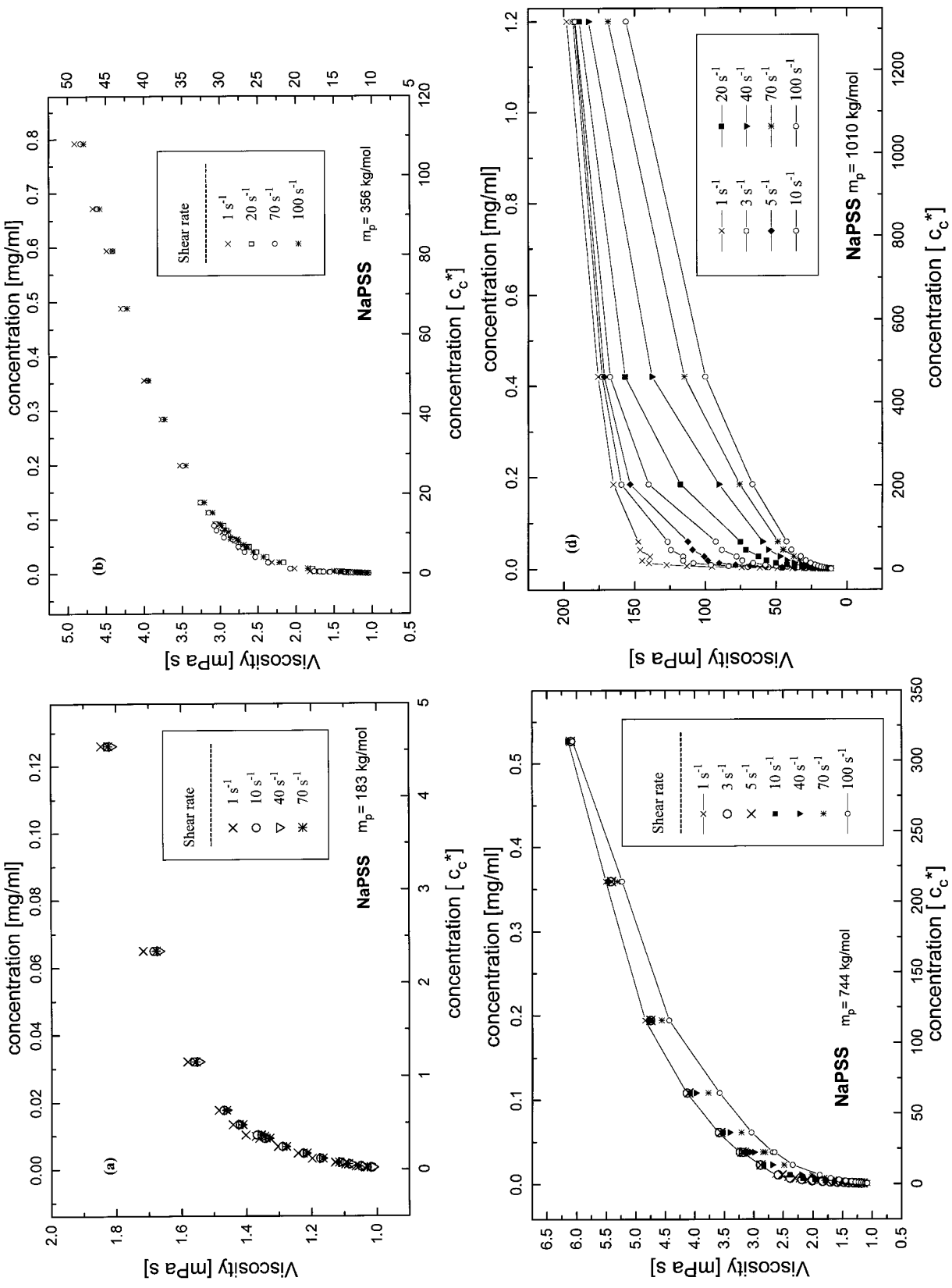

Fig. 7. Concentration dependence of the viscosity derived from the data of Figures 6a-d.

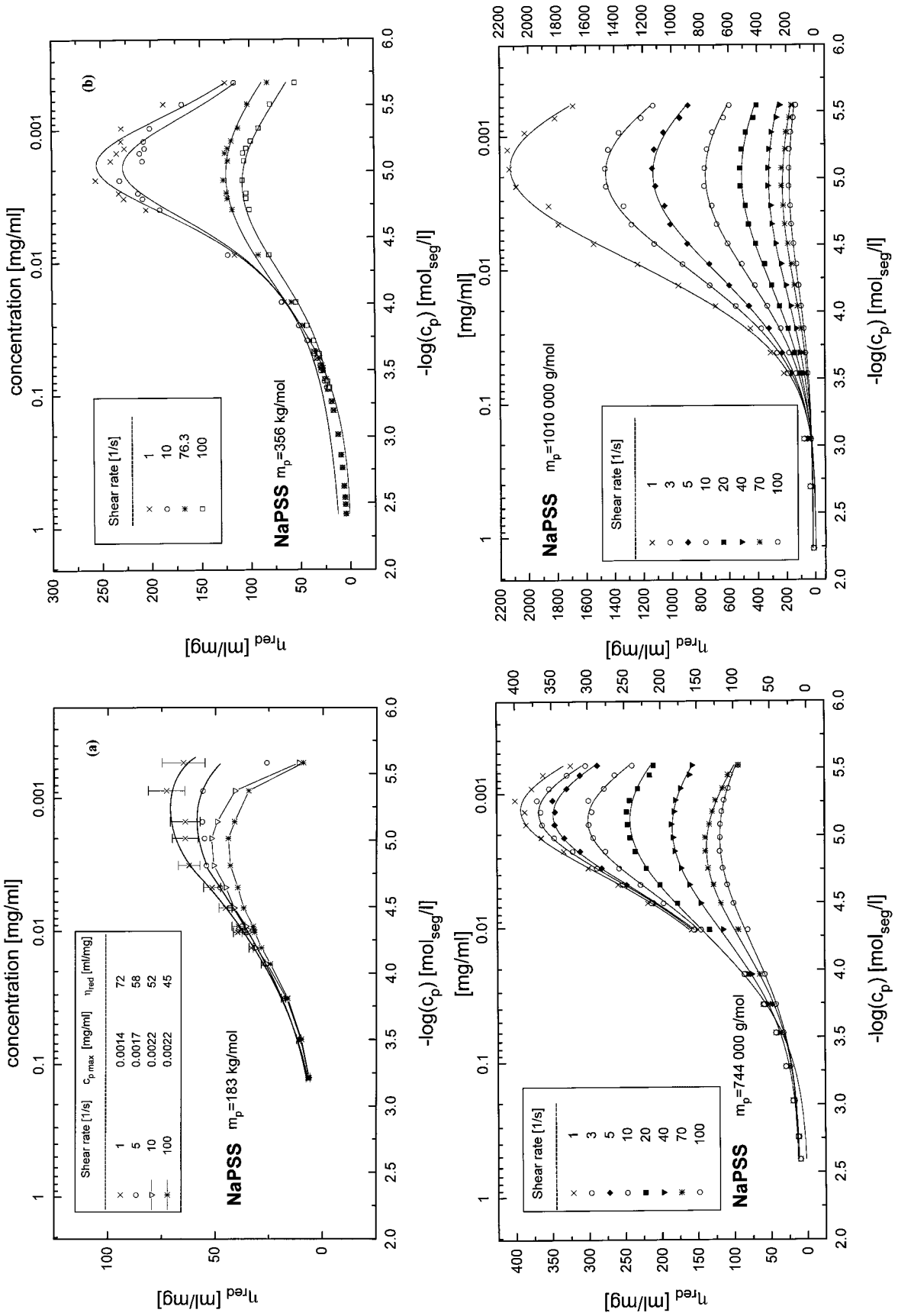

Fig. 8. The reduced viscosity derived from the data of Figures 6a-d.

We wish to thank Professors G. Maret and U. Steiner (Faculty of Chemistry) for useful discussions, and B. Nadig for technical assistance. This work was financially supported by the Deutsche Forschungsgemeinschaft (SFB 306).

References

1. S. Förster, M. Schmidt, Adv. Polym. Sci. **120**, 50 (1995).
2. M. Nierlich, C.E. Williams, F. Boué, J.P. Cotton, M. Daoud, B. Farnoux, G. Jannink, C. Picot, M. Moan, C. Wolff, M. Rinaudo, P.G. de Gennes, J. Phys. France **40**, 701 (1979).
3. F. Nallet, G. Jannink, J.B. Hayter, R. Oberthür, C. Picot J. Phys. France **44**, 87 (1983).
4. T. Kanaya, K. Kaji, R. Kitamazu, J.S. Higgins, B. Farago, Macrom. **22**, 1356 (1989).
5. N. Ise, T. Okubo, S. Kunngi, H. Matsuoka, K. Yamamoto, Y. Ishii, J. Chem. Phys. **81**, 3294 (1984).
6. K. Kaji, H. Urekawa, T. Kanaya, R. Kitamaru, J. Phys. France **49**, 993 (1988).
7. M. Drifford, J.P. Dalbiez J. Chem. Phys. **88**, 5368 (1984).
8. R. Krause, E.E. Maier, M. Deggelmann, M. Hagenbüchle, S.F. Schulz, R. Weber, Physica A **160**, 135 (1989).
9. C. Johner, H. Krause, S. Batzill, C. Graf, M. Hagenbüchle, C. Martin, R. Weber, J. Phys. II France **4**, 1571 (1994).
10. J. Hayter, G. Janninck, E. Brochard-Wyart, P.G. de Gennes, J. Phys. Lett. France **41**, L451 (1980).
11. R.G. Smits, M.E. Kuil, M. Mandel, Macrom. **27**, 5599 (1994).
12. S. Gosh, R.M. Peitszch, W.F. Reed, Biopolymers **32**, 1105 (1992).
13. J. Cohen, Z. Priel, J. Chem. Phys. **88**, 7111 (1988) and Macromol. **22**, 2356 (1989).
14. J. Yamanaka, H. Matsuoka, H. Kitano, M. Hasegawa, N. Ise, J. Am. Chem. Soc. **112**, 587 (1990).
15. H. Vink, Polymer **33**, 3711 (1992).
16. J.L.M.S. Ganter, M. Milas, M. Rinaudo, Polymer **33**, 113 (1992).
17. T. Palberg, W. Härtl, U. Wittig, M. Versmold, M. Würth, J. Phys. Chem. **90**, 8801 (1992).
18. M. Deggelmann, T. Palberg, M. Hagenbüchle, E.E Maier, R. Krause, C. Graf, R. Weber, J. Coll. Int. Sci. **143**, 318 (1990).
19. W.F. Reed, J. Chem. Phys. **101**, 2515 (1994).
20. Diplomarbeit Luxemburger R., Universität Konstanz (1996), unpublished.
21. M. Hagenbüchle, B. Weyerich, M. Deggelmann, C. Graf, R. Krause, E.E. Maier, S.F. Schulz, R. Klein, R. Weber, Physica A **169**, 32 (1990).
22. E.E. Maier, R. Krause, M. Deggelmann, M. Hagenbüchle, R. Weber, Macrom. **25**, 1125 (1992).
23. B. Weyerich, B.D. d'Aguanno, E. Canessa, R. Klein, Faraday Disc. Chem. Soc. **90**, 245 (1990).
24. Shew Chwen-Yang, Yethiraj Arun, J. Chem. Phys. **106**, 5706 (1997).
25. P.G. De Gennes, P. Pincus, R.M. Velasco, J. Phys. France **37**, 1461 (1976).
26. M. Benmouna, G. Weill, H. Benoit, A.Z. Akcasu, J. Phys. France **43**, 1679 (1982).
27. R. Koyama, Physica B **120**, 418 (1983).
28. R. Koyama, Macrom. **17**, 194 (1984).
29. R. Koyama, Macrom. **19**, 178 (1986).
30. M.J. Stevens, K. Kremer, J. Chem. Phys. **103**, 1669 (1995).
31. P.W. Pusey, R.J.A. Tough, in: *Dynamic Light Scattering: Application of Photon Correlation Spectroscopy*, edited by R. Pecora (Plenum Press, New York, London, 1985).
32. J.B. Berne, R. Pecora, *Dynamic Light Scattering* (Wiley, New York, 1976).
33. E. Overbeck, Diplomarbeit Universität Konstanz, 1995, unpublished.
34. C. Graf, M. Deggelmann, M. Hagenbüchle, H. Kramer, R. Krause, C. Martin, R. Weber, J. Chem. Phys. **95**, 6284 (1991).
35. W. Hess, R. Klein, Adv. Phys. **32**, 173 (1983).